

# Finite-element Modeling of Femur Based on CT Data and a Preliminary Study of Stress Distribution of CCB Hip Prosthesis After Implantation\*

LÜ Da-Wei, CAI Xu\*\*, WANG Yan\*\*

(General Hospital of PLA, Beijing 100853, China)

**Abstract** Finite element method (FEM) models have been developed. Here a loading is applied and the stress distribution is detected, and then a comparative study is carried out under different conditions. Data are provided to optimize the design of CCB hip prosthesis. FEM models of femur and CCB hip prosthesis are established; the condition of monopod support is imitated and the stress distributions are detected and compared under different conditions using three-dimension finite element analysis software Ansys5.7. The data are treated with SPSS Statistics 17.0 and presented in line chart. Result showed that (1) Connection by cancellous bone will increase stresses around the hole; (2) Holes on the lateral side can lower the maximum stress on the lateral side slightly; (3) Shortening the length of the prosthesis can enlarge the biomechanical effect of the design; (4) Stress around the lower hole is always higher than the upper one, and the direction of the force in the corresponding position basically remains the same.

**Key words** FEM, biomechanics, hip prosthesis

**DOI:** 10.3724/SP.J.1206.2011.00016

Arthroplasty is an effective measure to treat some severe joint diseases. Joint diseases resulting from degenerative changes prevail with aging, and arthroplasty is accepted as the ultimate method to solve these problems. Nevertheless aseptic loosening affects clinical effect and has not been properly solved among the cementless prosthesis in use. Recent animal experiments found that the range and depth of bone ingrowth on the surface of prosthesis was limited<sup>[1]</sup>. Prompting bone ingrowth and enlarging binding area would enhance stability. Thus many studies are concentrated on this topic. CCB hip prosthesis designing a hollow part on the lateral side of the stem introduced tissue engineering concept, using scaffold combined with BMP to induce bone formation. The purpose of this study is to identify the function of this special design and illustrate the biomechanical properties, furthermore provide basic information to improve the design.

## 1 Materials and methods

### 1.1 Experiment set-up

A CT picture in this study is provided by an autonomous robot & mechatronic system of BeiHang University, with an interval of 0.5 mm and 895 pieces in all. Computer system configuration is as follows: CPU Potium IV/2.4G, memory size 2G. Relative software includes Ansys 5.7, Geomagic8.0. And data concerning geometric properties and biomechanics of materials are provided by Baimtec Material Co, Ltd.

\*This work was supported by a grant from The National Natural Science Foundation of China (30471755).

\*\*Corresponding author.

Tel: 86-10-66939236, E-mail: 301wangyan@sina.com

Received: March 31, 2011 Accepted: June 13, 2011

The prosthesis is made of Ti-6Al-4V alloy. The elastic module is 116 GPa and the Poisson ratio is 0.3. And the model of femur is treated as liner elastic material composed of cortical bone and cancellous bone. The elastic modules of cortical and cancellous bone are 17.6 GPa and 300 MPa respectively. The Poisson ratio is 0.29<sup>[2]</sup>. The prosthesis model and prosthesis in use are shown in Figure 1 and 2.



Fig. 1 The model of the hip prosthesis



Fig. 2 The product in use

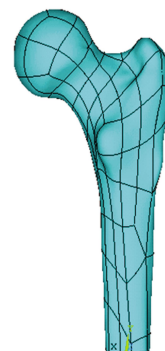


Fig. 3 The middle-upper part of the femur model

**1.2.2** A FEM model of CCB hip prosthesis was simplified, retaining the hollow part design and making two holes on the lateral side with diameter of 5 mm as shown in Figure 4 and 5. Then shortened-stem design was adopted to further investigate the effect. The stem was shortened to 80 mm, retaining the hollow part design with a diameter of 10 mm as shown in Figure 6 and 7.

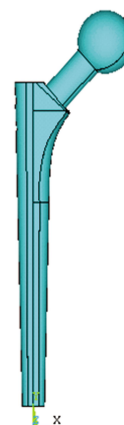


Fig. 4 The anterior-posterior view of the FEM model of the prosthesis

## 1.2 Experiment procedure

**1.2.1** A finite element method (FEM) model of femur was developed based on the data of CT. First, geometrical model was optimized using Geomagic8.0. Then polyhedra was blended using NURBS, and the model underwent surface reconstruction as shown in Figure 3. Through the interface between ANSYS and CAD system, this 3D graphic was transported to Ansys5.7 and inverted to an FEM model. This FEM model was meshing using solid45 unit<sup>[3-4]</sup>.

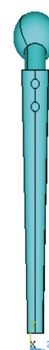


Fig. 5 The lateral view of the FEM model of the prosthesis

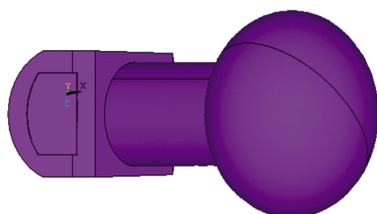


Fig. 6 The vertical view of the FEM model of the prosthesis

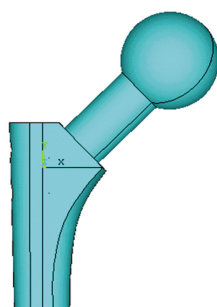


Fig. 7 The shortened design of the prosthesis

**1.2.3** The procedure and criterion of implantation strictly followed the standard step of hip arthroplasty<sup>[5]</sup>. Adopted strength theory of material is the fourth strength law. Ideal results of operation could achieve no relative motion between bone and prosthesis. The FEM model after implantation was made of 26 168 nodes and 111 315 elements in all as shown in Figure 8. And during computation coupling DOFS was adopted to simulate this condition as shown in Figure 9.

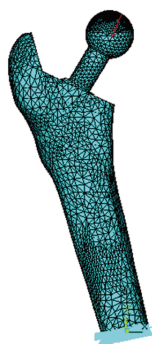


Fig. 8 Meshing the model after implantation

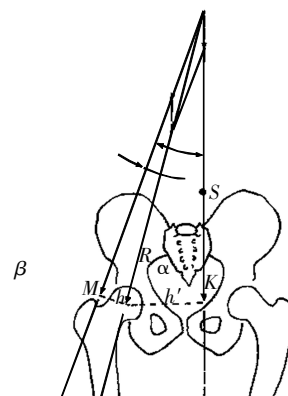


Fig. 9 Monopod support

The weight force of the body ( $K$ ) and the equilibrium force generated by the buttock muscles ( $M$ ) are composed and the resulting force ( $R$ ) acting upon the upper femoral extremity.

**1.2.4** Model loading. During the monopod support or walking, the force acting on the upper part of femur includes the weight force and the force generated by the buttock muscles. The mathematical analysis is made for monopod support<sup>[6-7]</sup>. We admit that the center of the femoral head is under the action of a concentrated load ( $R$ ) forming an angle of  $25^\circ$  with the axial of femur. This load is the resultant force of the body weight and the force developed by the hip muscles. Adopting that the body weight is 60 kg, and the load is  $3G$ , we postulate that:  $R = 3G = 3 \times 600 \text{ N} = 1800 \text{ N}$ .

### 1.3 Statistical analysis

The results were statistically analyzed using SPSS Statistics 17.0 and presented by diagrams.

## 2 Results and discussion

### 2.1 Analysis of force distribution

**2.1.1** Von Mises force distribution on frontal sections in different conditions after implantation. Stress concentrates on the end of the prosthesis, and the values of Von Mises force vary primarily in the range of  $200 \sim 500 \text{ MPa}$ . Figure 10 shows Von Mises force distribution on frontal sections of normal hip prosthesis. The stress conduction pattern and the maximum Von Mises force make no obvious difference between the normal hip prosthesis and CCB

hip prosthesis. Figure 11 shows Von Mises force distribution on frontal sections when the hollow part of CCB hip prosthesis has not connected with surrounding bone mass. After the hollow part connected with the surrounding bone mass, the stress conduction pattern and the maximum Von Mises force also don't change a lot. Figure 12 and 13 show Von Mises force distribution on frontal sections when the hollow part of CCB hip prosthesis connected with surrounding bone mass. In order to further investigate the effect of the design, then the Shortened-stem prosthesis has been adopted. Figures 14 and 15 show Von Mises force distribution on frontal sections of shortened stem. Stress still concentrates on the end the prosthesis, while the Von Mises force on the bone mass around the hole and the neck of prosthesis rises.

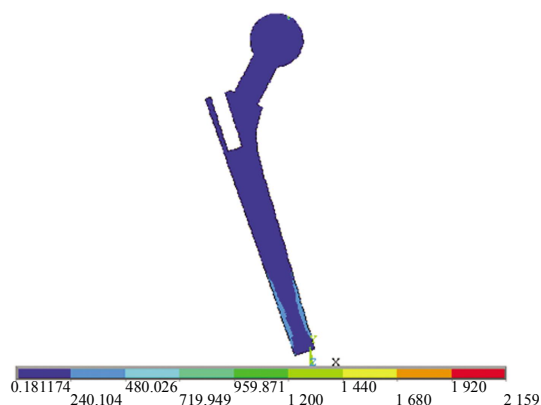


**Fig. 10** Von Mises force distribution on frontal section of normal prosthesis

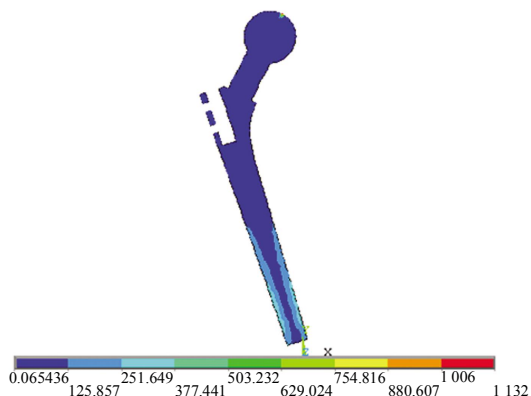


**Fig. 11** Von Mises force distribution on frontal section of the prosthesis

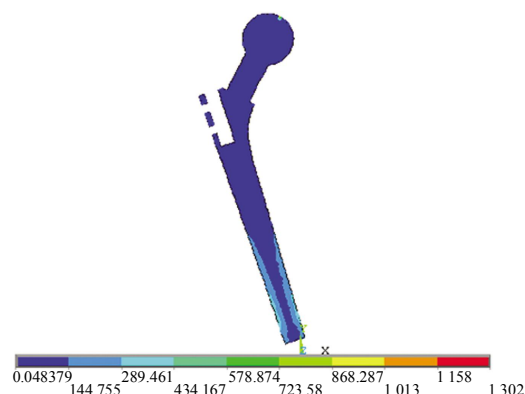


**Fig. 12** Von Mises force distribution on frontal section of the prosthesis when the hollow part connecting with surrounding bone mass through cancellous bone formation

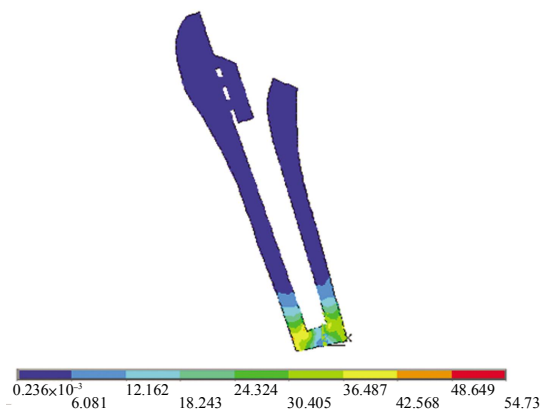


**Fig. 13** Von Mises force distribution on frontal section of the bone mass when the hollow part connecting with surrounding bone mass through cancellous bone formation

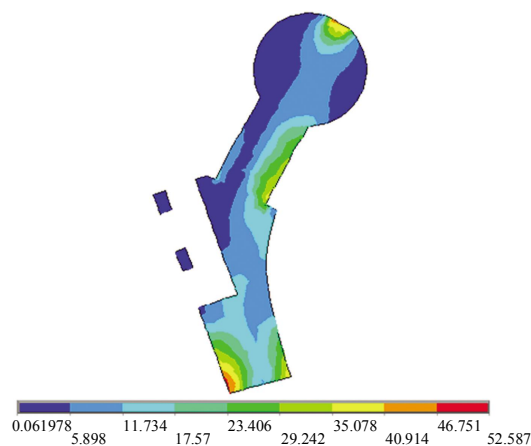


**Fig. 14** Von Mises force distribution on frontal section of the shortened prosthesis

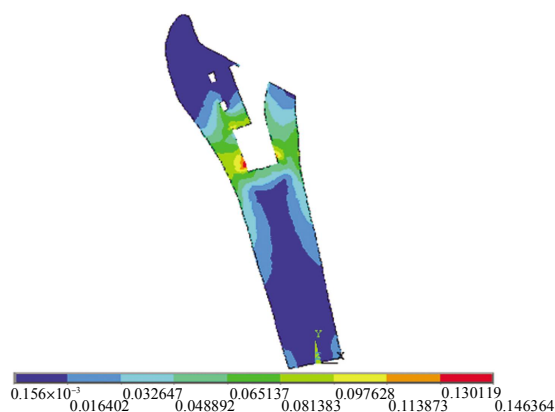


**Fig. 15** Von Mises force distribution on frontal section of the bone mass when the hollow part connecting with surrounding bone mass through cancellous bone formation

**2.1.2** Main tension distribution on the lateral side and around the holes of the CCB hip prosthesis in different conditions after implantation. Figure 16 shows that main tension on the lateral side of prosthesis before and after the hollow part is connected with surrounding bone mass. The shapes of the curves are the same, with most part overlapped. Figures 17 and 18 show main tension around the holes of prosthesis before and after the hollow part is connected with

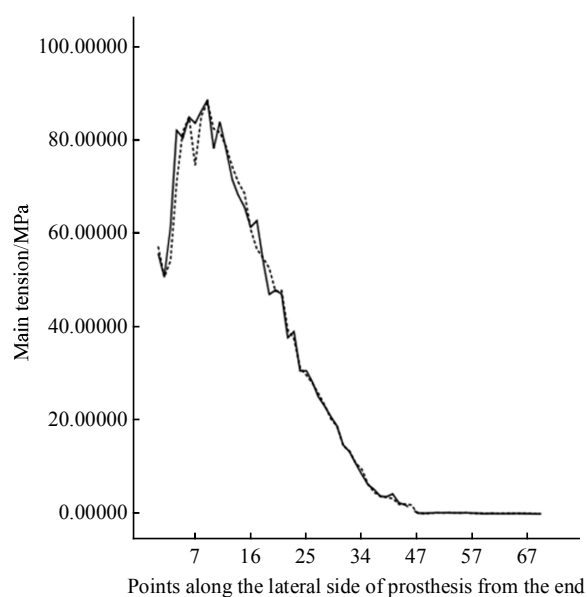


**Fig. 16** Main tension developed on the lateral side of the prosthesis before and after connect  
— : Before connect; - - - : After connect.

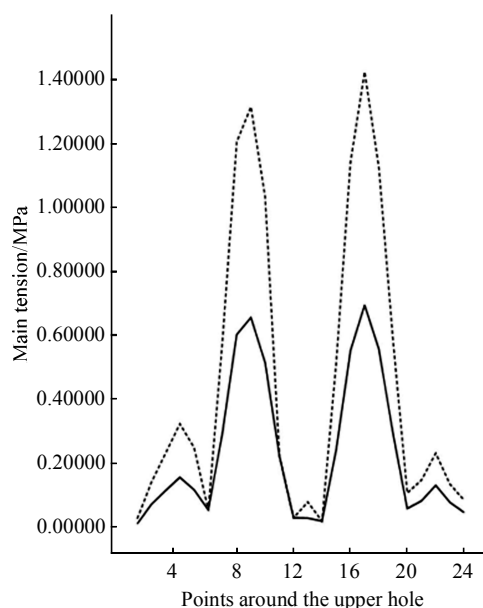


**Fig. 17** Main tension developed around the upper hole before and after connect  
— : Before connect; - - - : After connect.

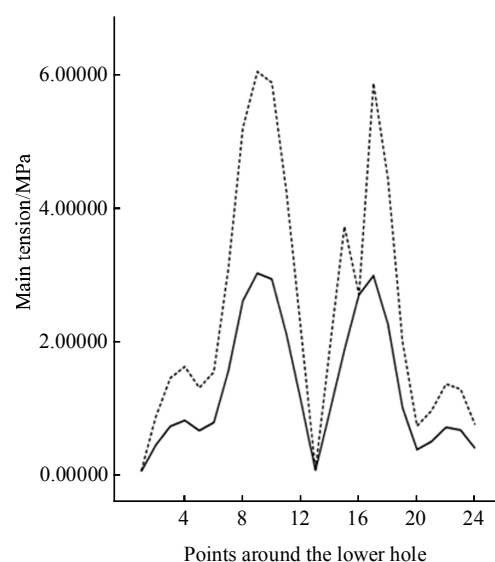


**Fig. 18** Main tension developed around the lower hole before and after connect  
— : Before connect; - - - : After connect.

surrounding bone mass. The shapes of the curves are almost the same, while the maximum tension is approximately doubled after the hollow part connected with the surrounding bone mass.

## 2.2 Assessment of the effect on mechanical conducting

**2.2.1** The alteration of Von Mises force distribution after opening holes on the lateral side. The maximum Von Mises force on the lateral side of normal hip prosthesis is 382.525 MPa, and the maximum Von Mises force on the other side is 361.089 MPa. The maximum Von Mises force on the lateral side of CCB hip prosthesis is 343.843 MPa, and the maximum Von Mises force on the other side is 326.921 MPa. Under both conditions, the Von Mises force around the holes remains  $1 \sim 10^{-1}$  MPa and makes no obvious difference. The yield strength of titanium alloy is 896 MPa, thus the experimental condition of the study can not cause any harm.

**2.2.2** The alteration of Von Mises force distribution after the hollow part connecting with the surrounding bone mass. The distribution of Von Mises force on the lateral side before and after connecting does not make much difference. The Von Mises force around the holes remains  $1 \sim 10^{-1}$  MPa and is approximately doubled after connecting. The force around the lower hole is always greater than that around the upper hole. The upper part of the prosthesis displays tension, while the lower part displays stress.

**2.2.3** The alteration of Von Mises force distribution after shortening the stem of CCB hip prosthesis. The Von Mises force on both sides reduces greatly, the maximum on the lateral side is 62.501MPa, and the maximum on the other side is 43.933MPa. The force around the hole increases greatly, however the Von Mises force curve pattern makes no obvious difference.

## 2.3 Discussion

Hip prostheses are abundant in variety, which fall into two general categories in terms of the fixation method: cemented and cementless. The fixation theory of cementless hip arthroplasty mainly relies on press-fit technique and the connection between bone mass and the porous or bio-ceramic surface of hip prostheses to achieve initial and long-term stability. However, long-term follow-up results show the existing aseptic loosening and the limited bone ingrowth among most of porous surface of the hip prostheses, with osseointegration percentage ranging from 6% to 20%. While ultra-high molecular polyethylene wear debris causes osteolysis; stress shielding causes bone resorption; total hip arthroplasty causes the loss of tensile stress around the greater

trochanter of femur; these entire problem can lead to the destruction of bone structure. Therefore, retaining the original hypothesis of cementless hip prosthesis, it is necessary to introduce some new conception.

FEM has distinct advantages in evaluating mechanical properties and optimizing design of medical equipment. Experiment of FEM has many advantages, such as spending less time, consuming lower expenses, having a possibility to imitate comprehensive conditions and to detect more parameters concerning mechanical properties, and especially, its high repeatability<sup>[8]</sup>. Therefore, it is also commonly adopted in developing new equipment. Recent researches in China and abroad are listed as follows: (1) In Viceconti's study<sup>[9]</sup> about primary stability of an anatomical cementless hip stem, many factors including the mechanical quality of the host bone, the presence of gaps around the bone-implant interface, the body weight of the patient, and the size of the implant were assessed; (2) In another study carried out by Sakai<sup>[10]</sup>, a concept of micromotion area was proposed and analyzed mechanical properties of different stems.

The original design concept of CCB hip prosthesis includes two aspects: one is concerning mechanics, and the other is on tissue engineering. The mechanical conducting form remains stress concentration at the end of the stem. The hollow part connecting with bone mass through cancellous bone formation does not change this pattern.

The advantages and disadvantages of CCB hip prosthesis are summarized as follows: the advantages include reducing bone loss, inducing bone formation and decreasing the maximum stress slightly; the disadvantage is no conspicuous effect on mechanical conducting. It should be noted that the yield strength of titanium alloy allows some amendments to the design, and the material connecting bone mass to the hollow part is not pure cancellous bone, which contains some dense bone, supported by previous study, thus the actual function in the body would be more conspicuous.

## References

- [1] Cai X. A biologically compounded hollow part artificial joint. *J World Medical Instrument*, 2004, **10**(2): 12-15
- [2] 罗成刚, 龚宪生. 近端股骨的非均匀及各向异性有限元模型. *重庆大学学报*, 2004, **27**(2): 20-23  
Luo C G, Gong X S. *J Chongqing University*, 2004, **27**(2): 20-23

- [3] 刘安庆, 张银光, 王春生. 人股骨生物力学特性的有限元分析. 西安医科大学学报, 2001, **22**(3): 242-244  
Liu A Q, Zhang Y G, Wang C S. J Xi'an Medical University, 2001, **22**(3): 242-244
- [4] Hutton D V. Fundamentals of Finite Element Analysis. Wu J H, Abbrev. Chongqing: Chongqing University Press, 2007: 3
- [5] 毛宾尧. 髋关节外科学. 北京: 人民卫生出版社, 1998: 36  
Mao B Y. The Surgery of The Hip Joint. Beijing: People's Health Press, 1998: 36
- [6] 戴尅戎, 王以进. 骨骼系统的生物力学基础. 北京: 学林出版社, 1985: 17  
Dai K R, Wang Y J. Basic Mechanics of Skeletal System. Beijing: Academic Press, 1985: 17
- [7] Wang T Y, Jiang F C, Wang X S. Human hip contact force analysis. Mechanics in Engineering, 2005, **27**(2): 67-69
- [8] 陶祖荣. 生物力学导论. 天津: 天津科技翻译出版公司, 2000: 87-88  
Tao Z L. Introduction to Biomechanics. Tianjin: Tianjin Science & Technology Translation & Publishing Co., 2000: 87-88
- [9] Viceconti M, Brusi G, Pancanti A, *et al.* Primary stability of an anatomical cementless hip stem: a statistical analysis. J Biomech, 2006, **39**(7): 1169-1179
- [10] Sakai R, Itoman M, Mabuchi K. Assessments of different kinds of stems by experiments and FEM analysis: appropriate stress distribution on a hip prosthesis, Clin Biomech (Bristol, Avon), 2006, **21**(8): 826-833

## 基于 CT 的股骨有限元模型的建立及髋关节中空多孔假体植入后受力分布的初步研究 \*

吕大伟 蔡 胥 王 岩 \*\*

(中国人民解放军总医院骨科, 北京 100853)

**摘要** 利用有限元分析的方法, 对髋关节中空多孔假体植入后的受力分布改变进行研究, 为改进中空多孔人工关节假体的设计提供依据. 建立了股骨和假体三维有限元模型, 应用有限元分析软件 Ansys5.7 模拟单腿负重状态, 考察应力分布并进行比较. 使用 SPSS Statistics 17.0 软件进行分析处理, 绘制折线图. 结果表明: a. 开孔后张力侧最大压应力有所减小, 开孔部位的应力水平变化不明显. b. 与周围骨质形成连接后孔缘局部应力增加, 张力侧受力改变不明显. c. 短柄假体受力模式仍为远端应力集中; 张力侧应力减小, 开孔部位应力明显增加. d. 下孔受力均大于上孔, 受力方向基本一致.

**关键词** 有限元分析, 生物力学, 髋关节假体

**学科分类号** R318.01

**DOI:** 10.3724/SP.J.1206.2011.00016

\* 国家自然科学基金资助项目(30471755).

\*\* 通讯联系人.

Tel: 010-66939236, E-mail: 301wangyan@sina.com

收稿日期: 2011-03-31, 接受日期: 2011-06-13